Available online at www.sciencedirect.com
SCIENCE DIRECT
Journal of Membrane Science 277 (2006) 75–84
journal of MEMBRANE SCIENCE
www.elsevier.com/locate/memsci

Combined models of membrane fouling: Development and application to microfiltration and ultrafiltration of biological fluids

Glen Bolton *, Dan LaCasse, Ralf Kuriyel

Millipore Corporation, 32 Wiggins L2B, Bedford, MA 01730, USA

Received 23 August 2004; received in revised form 22 November 2004; accepted 22 December 2004
Available online 1 December 2005

Abstract

Membrane capacity during the filtration of biotech process streams is typically limited by fouling, which can occur by pore blocking, pore constriction, caking or a combination of the mechanisms. In this study five new fouling models that accounted for the combined effects of the different individual fouling mechanisms were generated. Explicit equations were derived from Darcy's law that related pressure to time during constant flow operation and volume to time during constant pressure operation. The models used two fitted parameters and reduced to the individual models when one mechanism dominated. The applicability of the models to data for the sterile filtration of IgG and the viral filtration of BSA was tested. The combined caking and complete blockage model was the most useful, as it was able to provide good fits of both data sets, and provide good fits of each of the other individual model predictions. The cake-complete model will provide good fits of a broad range of curves where the flux declines in a manner between the extremes of cake filtration and complete blocking. The combined cake-standard and cake-intermediate models also provided good data fits and may be applicable to systems where these models are consistent with the experimentally observed fouling mechanisms.

Keywords: Membrane; Fouling; Blocking; Microporous; Filtration

1. Introduction

Sterilizing grade membranes are used throughout biotech purification processes to remove bacteria from fermentation media, buffers and process streams. Additionally there is an increasing use of filters for the removal of viruses from these streams. The membrane area required by these process steps can be determined by limitations in the membrane permeability, membrane capacity, or a combination of the two. For operations run at a fixed trans-membrane pressure, capacity is defined as the amount of fluid per membrane area that can be processed until the flux declines to a set fraction of the initial flow. For operations run at a fixed flow rate, capacity is determined when the trans-membrane pressure increases to some set multiple of the initial value.

Fouling of a membrane can occur by deposition of particles inside or on top of the membrane [1,2]. There are four mechanistic models that are typically used to describe fouling. Complete blocking assumes that particles seal off pore entrances and prevent flow. Intermediate blocking is similar to complete blocking but assumes that a portion of the particles seal off pores and the rest accumulate on top of other deposited particles. Cake filtration occurs when particles accumulate on the surface of a membrane in a permeable cake of increasing thickness that adds resistance to flow. Standard blocking assumes that particles accumulate inside membranes on the walls of straight cylindrical pores. As particles are deposited, the pores become constricted and the permeability of the membrane is reduced. Each of these mechanisms have been used individually or in combinations to explain experimental observations. Bowen and Gan [3] observed that BSA fouled microporous aluminum oxide, PVDF, and polycarbonate membranes internally because stirring of the system had no effect on flux decline and because the standard blocking mechanism provided good curve fits. Marshall et al. concluded that proteins can foul microporous membranes both by deposition within the membrane pores and deposition on the membrane surface [4]. Hlavacek and Bouchet [5] fit the intermediate, complete and standard models to data for the fouling of microporous

* Corresponding author. Tel.: +1 978 247 1601; fax: +1 978 246 2604.
E-mail addresses: Gbolton@Wyeth.com (G. Bolton), DPLaCasse@Wyeth.com (D. LaCasse), Ralf_Kuriyel@Pall.com (R. Kuriyel).

0376-7388/$ – see front matter © 2005 Elsevier B.V. All rights reserved.
doi:10.1016/j.memsci.2004.12.053

track-etched polycarbonate, cellulose, and PVDF membranes by BSA and found that the intermediate model provided the best fits. Tracey and Davis [6] found that data for the fouling of microporous track-etched membranes by BSA could be fit initially by either the standard or complete model and subsequently by the cake model. Bowen et al. [7] observed that the flux decline during the fouling of microporous track-etched membranes by BSA did not follow any of the individual fouling models and likely occurred through a combination of complete blocking, standard blocking, and cake formation. The results of the different studies indicate microporous membranes can foul by both surface and pore deposition and the mechanisms vary with system conditions.

A number of models of the effects of deposition of different particles sizes on the permeability of porous media have been developed. Particles can deposit due to inertial impaction, interception, sedimentation, electrostatic forces, diffusion and straining. A detailed description of these mechanisms and the models that have been developed to describe them is provided by Tien [8]. The particles that typically foul microporous membranes are too small to foul by impaction or sedimentation. Typically particles are strained, resulting in pore blockage or caking, or particles are adsorbed due to the effects of diffusion, interception, or electrostatic forces.

Recently a model was developed that used a two-stage mechanism to describe membrane fouling [9]. Fouling occurred initially through complete pore blocking. The deposited aggregates were assumed to be permeable. Flow through the blocked areas resulted in the deposition of a cake, reducing flux further. This was the first model that accounted for the combined effects of two fouling mechanisms. The model used three fitted parameters and an approximate solution was provided that allowed calculation of flux as a function of time without integrating. Plots of volume versus time during constant pressure operation or pressure versus time during constant flow operation were obtained by numerical integration of the relevant equations. The values of the fitted parameters were similar to the values obtained by independent experiments. The authors found this model provided good data fits and made accurate membrane sizing estimates for the fouling of microporous track-etched membranes by five proteins.

In this study the previous modeling work was expanded by using a new method to combine the four individual fouling mechanisms. The goal was to develop models that described combined-mechanism fouling with two fitted parameters and with explicit equations for constant flow and constant pressure operation. Five new fouling models that accounted for the combined effects of the different individual fouling mechanisms were derived from Darcy's law. Explicit equations were derived that related pressure to time during constant flow operation, and volume to time during constant pressure operation. The models all used two fitted parameters and reduced to the individual models in the absence of the second fouling mechanisms. The combined models were assessed through testing under constant pressure and constant flow modes with solutions of bovine serum albumin and human IgG. Bovine serum albumin was filtered through virus retention membranes and human IgG was filtered through sterilizing grade microporous membranes. The combined caking and complete blockage model was the most useful, as it was able to provide good fits of both data sets, and provide good fits of each of the other individual model predictions. The combined cake-standard and cake-intermediate models also provided good data fits and may be applicable to systems where these models are consistent with the experimentally observed fouling mechanisms.

2. Modeling

The flow rate Q can be calculated as a function of resistance R and membrane frontal area A using Darcy's law

$$Q = \frac{PA}{R\mu} \tag{1}$$

where P is the trans-membrane pressure and μ is the solution viscosity.

2.1. Standard blocking model

In the standard model, membranes have straight cylindrical pores that decline in radius as solid matter accumulates on the pore walls [1,2]. The resistance can be calculated as a function of volume processed using Eq. (2), or time using Eq. (3)

$$R = R_0\left(1 - \frac{K_s V}{2}\right)^{-2} \tag{2}$$

$$R = R_0\left(1 + \frac{K_s J_0 t}{2}\right)^{2} \tag{3}$$

The volume can be calculated as a function of time from

$$V = \left(\frac{1}{J_0 t} + \frac{K_s}{2}\right)^{-1} \tag{4}$$

where J_0 is the initial flux and K_s is the standard blocking constant and has units of m^{-1}.

2.2. Complete and intermediate blocking models

When a membrane fouls by the complete or intermediate blocking mechanism a portion of the pores are unavailable for flow. The available membrane area declines with permeate volume in the complete model according to Eq. (5), and in the intermediate model according to Eq. (6) [2]

$$\frac{A}{A_0} = 1 - \frac{K_b}{J_0} V \tag{5}$$

$$\frac{A}{A_0} = \exp(-K_i V) \tag{6}$$

The constant K_b has units of s^{-1}, and K_i has units of m^{-1}. The equations are valid for both constant pressure and constant flow operation.

For constant trans-membrane pressure operations, the equations can be inserted into Darcy's law, Eq. (1), and integrated to derive equations for volume versus time. Eq. (7) describes

complete blocking and Eq. (8) describes intermediate blocking. These equations can be inserted into Eqs. (5) and (6) to calculate area as a function of time

$$V = \frac{J_0}{K_b}(1 - \exp(-K_b t)) \tag{7}$$

$$V = \frac{1}{K_i}\ln(1 + K_i J_0 t) \tag{8}$$

During constant flow rate operations, Eqs. (5) and (6) can be written in terms of time

$$\frac{A}{A_0} = 1 - K_b t \tag{9}$$

$$\frac{A}{A_0} = \exp(-K_i J_0 t) \tag{10}$$

Eqs. (9) and (10) can be inserted into Eq. (1) to obtain pressure as a function of time.

2.3. Cake filtration model

In the cake filtration model the resistance to flow is increased by the presence of a cake layer on the membrane surface. The total resistance R will be the sum of the membrane resistance and the cake resistance. This can be calculated as a function of volume by Eq. (11) and time by Eq. (12)

$$\frac{R}{R_0} = (1 + K_c J_0 V) \tag{11}$$

$$\frac{R}{R_0} = (1 + 2K_c J_0^2 t)^{1/2} \tag{12}$$

where K_c has units of s/m^2. Eq. (13) describes volume as a function of time

$$V = \frac{1}{K_c J_0}\left(\sqrt{1 + 2K_c J_0^2 t} - 1\right) \tag{13}$$

2.4. Combined models of membrane fouling

2.4.1. Constant pressure

To account for the combined effects of filtration area loss and caking, a new combined fouling model was developed. This was done by combining the loss of area predicted by the complete model with the increase in resistance predicted by the cake filtration model. Darcy's law was used to calculate the flux under constant pressure conditions. The flux $J = Q/A_0$

$$\frac{J}{J_0} = \frac{R_0 A}{R A_0} \tag{14}$$

In this model it was assumed that cake formation and complete pore blockage occur simultaneously. Cake forms on the membrane area that is not blocked. Complete blockage can occur on portions of the membrane area where a cake has formed. There is no flux through blocked membrane area. This is illustrated schematically in Fig. 1. Flux can be reduced, therefore, through a reduction in area through complete blockage or an increase in resistance through caking.

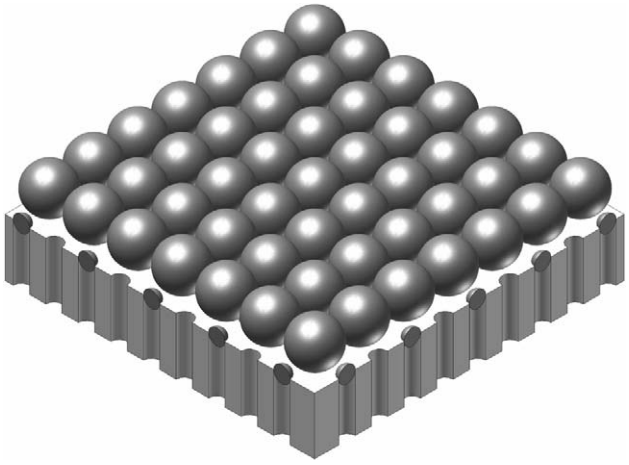

Fig. 1. Illustration of a cylindrical pore membrane fouling due to the combined effects of complete blockage and caking. Pores are blocked by small particles as larger particles form a cake above the membrane.

The resistance resulting from cake formation can be described either in terms of permeate volume, Eq. (11), or time, Eq. (12). Eq. (11) is not valid in this case because the permeate volume is defined relative to the available membrane area which is declining over the course of the run. If the equation for cake resistance in terms of volume processes was used, it would assume that there was a thin cake evenly distributed over the membrane. The cake will be thicker however over the unblocked pores than the blocked pores at the end of the run. The cake will form over the unblocked pores at the same rate with respect to time whether or not adjacent pores are blocked. Eq. (12) is still valid for the area that remains available.

The decrease in available membrane area can be described either in terms of permeate volume or time. The complete blocking will occur at a slower rate with respect to time due to the resistance of the cake. The equation for area as a function of time therefore cannot be used. The equation for complete blocking as a function of permeate volume, Eq. (5), will be valid in the presence of the cake. The flux equation with combined cake filtration-complete blocking is obtained by inserting Eqs. (12) and (5) into Eq. (14)

$$\frac{J}{J_0} = \left(1 - \frac{K_b V}{J_0}\right)(1 + 2K_c J_0^2 t)^{-1/2} \tag{15}$$

Eq. (15) can be integrated to solve for volume as a function of time

$$V = \frac{J_0}{K_b}\left(1 - \exp\left(\frac{-K_b}{K_c J_0^2}\left(\sqrt{1 + 2K_c J_0^2 t} - 1\right)\right)\right) \tag{16}$$

The combined cake-complete model was tested to determine if it provided the same results as the individual models when one mechanism dominates. When K_c is low, flux decline is caused mainly by complete blocking. In this case Eq. (16) reduces to the form of the complete blocking model after a Taylor expansion of the square root term for small values of K_c: $\sqrt{1+x} = 1 + x/2$.When K_b is low, fouling is caused mainly by cake filtration. In this case Eq. (16) reduces to the form of the cake filtration model after a Taylor expansion of the exponent term for small

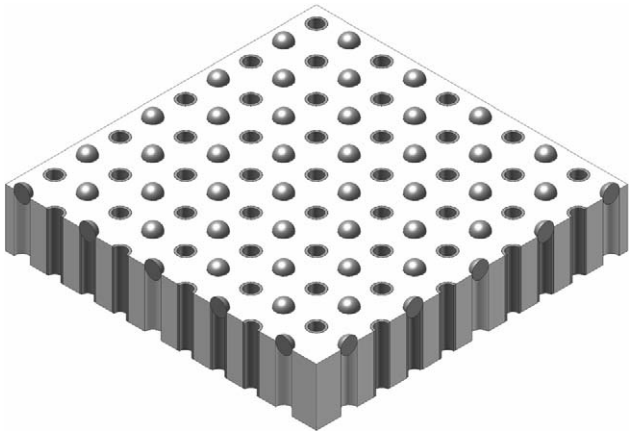

Fig. 2. Illustration of a cylindrical pore membrane fouling due to the combined effects of complete and standard blocking. Pores are constricted by solid matter accumulating evenly along the pore walls until the pores are blocked by small particles.

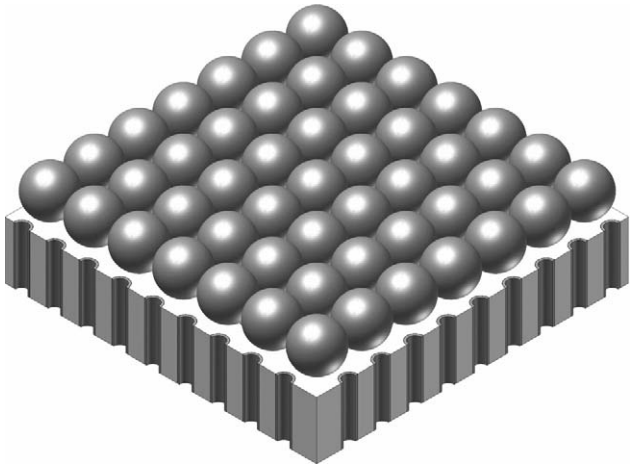

Fig. 3. Illustration of a cylindrical pore membrane fouling due to the combined effects of caking and standard blocking. Pores are constricted by solid matter accumulating evenly along the pore walls as large particles form a cake above the membrane.

values of K_b: $\exp(x) = 1 + x$. The confirmation of the expected results at the limits indicates the models are self-consistent.

The combined cake-complete model idealizes fouling as occurring by the independent effect of complete blocking and caking. This could occur if caking and pore blockage are caused by distinct species. It is possible that caking is caused by large particles that are excluded from the membrane and pore blockage is caused by smaller particles that are able to go through the cake and be retained in the membrane pores. In practice it is likely that the two fouling mechanisms will be coupled. For example, it is possible that as the pores become blocked the ability of the membrane to pass plugging species will be reduced and more cake will build up on the membrane surface. In this case caking will occur later in the filtration run. It is also possible that any cake that is formed will be retentive to fouling species and reduce the amount of pore blockage that will occur. In this case there will be less pore blockage occurring later in the run. The combined cake-complete model in effect provides complete blocking and cake filtration parameters that are average values for the length of the run.

It is not possible to obtain an equation that will allow calculation of volume as a function of flux with the cake-complete model. To determine the filtrate volume as a function of percent flux decline – for example, the volume after the flux has declined 75% from its initial value – it is necessary to solve Eq. (15) numerically.

It is possible using a similar technique to create a combined intermediate blocking-cake filtration model. Eq. (17) can be used to calculate volume as a function of time

$$V = \frac{1}{K_i} \ln\left(1 + \frac{K_i}{K_c J_0}((1 + 2K_c J_0^2 t)^{1/2} - 1)\right) \tag{17}$$

It is also possible to using a similar technique to create models that combine the standard blocking model with either the complete or intermediate blocking model. This is illustrated schematically in Fig. 2. The standard blocking equation for resistance as a function of time, Eq. (3) is valid in this case. Eq. (18) can be used to calculate volume as a function of time with the combined complete-standard blocking model

$$V = \frac{J_0}{K_b}\left(1 - \exp\left(\frac{-2K_b t}{2 + K_s J_0 t}\right)\right) \tag{18}$$

Eq. (19) can be used to calculate volume as a function of time with the combined intermediate-standard blocking model

$$V = \frac{1}{K_i} \ln\left(1 + \frac{2K_i J_0 t}{2 + K_s J_0 t}\right) \tag{19}$$

When K_i is low Eq. (19) reduces to the form of the standard blocking model after a Taylor expansion of the natural log term for small values of K_i: $\ln(1 + x) = x$. Eq. (19) reduces to the form of the intermediate model when K_s is zero. It can be shown using similar methods that Eqs. (17) and (18) reduce to their respective individual models when one mechanism dominates. Eqs. (17)–(19) will be applicable to the cases where the fouling is observed to occur by a specific combination of mechanisms. In practice Eqs. (17)–(19) do not span a wide range of flux decline rates and are not as useful as the combined cake-complete model. Typically the best fits occur when one of the two mechanisms dominates, in which case the combined equations do not offer much benefit over the individual models.

A model of the combined effects of pore constriction and caking was developed. In this case the available membrane area will not decline over the course of the run. For constant pressure operations Darcy's law can be reduced to Eq. (20)

$$\frac{J}{J_0} = \frac{R_0}{R} \tag{20}$$

The resistance after fouling can be calculated by adding the resistance from standard blocking to the resistance from cake formation. This is illustrated schematically in Fig. 3. The equations for resistance as a function of time cannot be used because the amount of cake fouling or standard blocking at any time will depend on the total resistance. In this case the extent of fouling by the two mechanisms will only depend on the volume processed and the equations for resistance as a function of volume

can still be used. The flux will be described by Eq. (21)

$$\frac{J}{J_0} = \left(\left(1 - \frac{K_s V}{2}\right)^{-2} + K_c J_0 V\right)^{-1} \tag{21}$$

Eq. (21) can be integrated to determine time as a function of volume

$$t = \frac{1}{(K_s V - 2)}\left(\frac{K_s K_c V^3}{2} - K_c V^2 - \frac{2V}{J_0}\right) \tag{22}$$

Eq. (22) reduces to the equation for cake filtration when K_s is small, and reduces to the equation for standard blocking when K_c is small. Eq. (22) can be used to calculate volume as a function of time numerically. It is also possible to solve Eq. (22) for volume as a function of time [10]

$$V = \frac{2}{K_s}\left(\beta\cos\left(\frac{2\pi}{3} - \frac{1}{3}\arccos(\alpha)\right) + \frac{1}{3}\right),$$
$$\alpha = \frac{8}{27\beta^3} + \frac{4K_s}{3\beta^3 K_c J_0} - \frac{4K_s^2 t}{3\beta^3 K_c} \quad \beta = \sqrt{\frac{4}{9} + \frac{4K_s}{3K_c J_0} + \frac{2K_s^2 t}{3K_c}}, \tag{23}$$

where α and β are dimensionless placeholders used to simplify Eq. (23). Eq. (23) is applicable when α is not near 1 or −1. This will be the case when neither of the two fouling mechanisms dominates. When the parameter values indicate that one fouling mechanisms dominates the corresponding individual model should be used.

The combined cake-standard model assumes that the two fouling mechanisms are independent and will occur throughout the run. This can occur if pore constriction is caused by small particles that can enter the membrane pores such as denatured protein monomers and caking is caused by large particles like protein aggregates that are excluded from the membrane. The small particles must not be retained by the cake above the membrane. It is likely however that some particles will be able to cause either pore constriction or caking. In this case it is likely pore constriction will occur initially, then more particles will be excluded from the membrane and form a cake. This is similar to the model of Ho and Zydney [9] where complete blockage occurs initially, followed by cake formation. It is possible that the cake will be retentive to particles and late in the run very little further pore constriction will occur. In this case the parameters used in the combined cake-standard model can be considered average values over the course of the run. A summary of the five new constant pressure combined fouling models, including the names, component mechanisms, equations, and fitted parameters is provided in Table 1.

2.4.2. Constant flow

When the flux rate is kept constant, the pressure increases as the membrane becomes fouled and Darcy's law reduces to Eq. (24)

$$\frac{P}{P_0} = \frac{RA_0}{R_0 A} \tag{24}$$

The fouling will occur both by loss of area through the complete blocking mechanism, and by increased resistance due to caking on the membrane.

The flux through the membrane area that has not become blocked will increase with time. An equation for flux versus time can be obtained by inserting the complete blocking equation for area as a function of time (9) into the equation for flux (1)

$$J' = \frac{J_0}{1 - K_b t} \tag{25}$$

This equation can be integrated to derive an equation that describes the amount of permeate volume that has gone through the available membrane area as a function of time

$$V' = \frac{-J_0}{K_b}\ln(1 - K_b t) \tag{26}$$

Here J' and V' are the flux and permeate volume relative to the available membrane area remaining, and not the total membrane area.

The caking will be observed as an increase in resistance of the membrane area available for filtration. This resistance will increase with the amount of permeate volume that has gone through that remaining area according to the cake filtration model

$$\frac{R}{R_0} = (1 + K_c J_0 V') \tag{27}$$

Eq. (26) can be inserted into Eq. (27) to determine the resistance as a function of time. This equation and the equation for area as a function of time (9) can then be inserted into Eq. (24) to determine pressure as a function of time

$$\frac{P}{P_0} = \frac{1}{(1 - K_b t)}\left(1 - \frac{K_c J_0^2}{K_b}\ln(1 - K_b t)\right) \tag{28}$$

This equation reduces to the equation for complete blocking when K_c is small and reduces to the equation for cake filtration when K_b is small. This equation will fit data where the pressure increases steeply and data where the pressure increases gradually, depending on the values of the fitted parameters. It will be more useful than models that can be made by combining the standard blocking equation with either the complete blocking model or the intermediate blocking model.

For the combined cake-standard blocking model, the resistance increases over the course of the run and the membrane area remain constant. The pressure can be calculated as a function of time using Eq. (29)

$$\frac{P}{P_0} = \left(\left(1 - \frac{K_s J_0 t}{2}\right)^{-2} + K_c J_0^2 t\right) \tag{29}$$

Eq. (30) allows calculation of pressure as a function of time using the combined intermediate blocking-cake filtration model

$$\frac{P}{P_0} = \exp(K_i J_0 t)\left(1 + \frac{K_c J_0}{K_i}(\exp(K_i J_0 t) - 1)\right) \tag{30}$$

Table 1
Summary of the five constant pressure combined fouling models

Model	Component mechanisms	Equation	Fitted parameters
Cake-complete (Eq. (16))	Cake filtration, complete blocking	$V = \frac{J_0}{K_b}\left(1 - \exp\left(\frac{-K_b}{K_c J_0^2}\left(\sqrt{1 + 2K_c J_0^2 t} - 1\right)\right)\right)$	K_c (s/m^2), K_b (s^{-1})
Cake-intermediate (Eq. (17))	Cake filtration, intermediate blocking	$V = \frac{1}{K_i}\ln\left(1 + \frac{K_i}{K_c J_0}((1 + 2K_c J_0^2 t)^{1/2} - 1)\right)$	K_c (s/m^2), K_i (m^{-1})
Complete-standard (Eq. (18))	Complete blocking, standard blocking	$V = \frac{J_0}{K_b}\left(1 - \exp\left(\frac{-2K_b t}{2 + K_s J_0 t}\right)\right)$	K_b (s^{-1}), K_s (m^{-1})
Intermediate-standard (Eq. (19))	Intermediate blocking, standard blocking	$V = \frac{1}{K_i}\ln\left(1 + \frac{2K_i J_0 t}{2 + K_s J_0 t}\right)$	K_i (m^{-1}), K_s (m^{-1})
Cake-standard (Eq. (23))	Cake filtration, standard blocking	$V = \frac{2}{K_s}\left(\beta\cos\left(\frac{2\pi}{3} - \frac{1}{3}\arccos(\alpha)\right) + \frac{1}{3}\right)$, $\alpha = \frac{8}{27\beta^3} + \frac{4K_s}{3\beta^3 K_c J_0} - \frac{4K_s^2 t}{3\beta^3 K_c}$, $\beta = \sqrt{\frac{4}{9} + \frac{4K_s}{3K_c J_0} + \frac{2K_s^2 t}{3K_c}}$	K_c (s/m^2), K_s (m^{-1})

Pressure as a function of time in the combined standard and complete blocking model will be described by Eq. (31)

$$\frac{P}{P_0} = \frac{1}{(1 - K_b t)\left(1 + \frac{K_s J_0}{2K_b}\ln(1 - K_b t)\right)^2} \tag{31}$$

Pressure as a function of time in the combined standard and intermediate blocking model will be described by Eq. (32)

$$\frac{P}{P_0} = \frac{\exp(K_i J_0 t)}{\left(1 - \frac{K_s}{2K_i}(\exp(K_i J_0 t) - 1)\right)^2} \tag{32}$$

The equations reduce to their respective component models at the limits where one fouling mode dominates. Eq. (29)–(32) will be applicable to the cases where the fouling is observed to occur by a specific combination of mechanisms. The equations however will not fit as wide a range of data as the combined cake-complete model and are therefore not as useful in general. A summary of the five new constant flow combined fouling models, including the names, component mechanisms, equations and fitted parameters is provided in Table 2.

3. Experimental

3.1. Proteins

Bovine serum albumin (BSA, Sigma, St. Louis, MO) was prepared at 2.5 mg/mL concentration in pH 7.2 PBS buffer (DF2314-15-0, Fisher Scientific, Hampton, NH). Human plasma IgG (Seracare, Oceanside, CA) was prepared in pH 7.2 PBS at a concentration of 10.0 mg/mL.

3.2. Membrane testing equipment: constant pressure

The fouling solution was contained in a pressure vessel (XX1100000, Millipore, Bedford, MA). Durapore PVDF based membrane with a nominal pore size rating of 0.22 μm was run at 10 psi during constant pressure tests. Viresolve 180, a PVDF composite membrane composed of a thin ultraporous layer on top of a thicker microporous layer, was run at 30 psi during constant pressure tests of virus filtration membranes. The solutions were filtered at constant pressure in 13 or 47 mm stainless steel holders (XX3001200, XX4404700, Millipore). An electronic balance aperture and a collection vessel were used to collect and measure the filtrate weight. The electronic balance consisted of a load cell (1042-3-I, Tedea Huntleigh, Covina, CA) that interfaced with a computer through a data acquisition board. The system was pressurized with air and a digital pressure gauge was used (2798K12, McMaster-Carr, Atlanta, GA).

Four 600 mL chambers were connected to the pressure source. The 47 mm membrane disks were wet with water, placed into the holders. The holders were vented to remove entrapped air. The feed solutions were added to their appropriate chambers and either 10 or 30 psi pressure was applied. The filtrate valves were then opened and data acquisition begun. The membrane surface area was 1.38×10^{-5} m^2. Data was collected every second for 1 h.

During constant flow tests, a peristaltic pump (L/S Precision #WF77911-20, Cole Parmer, Vernon Hills, IL) with 16 gauge tubing (06409-16, Cole Parmer) was used to pump 10 mg/mL IgG through the Durapore membrane in the 47 mm holders at 579 L/m^2 h.

4. Results

4.1. Constant pressure: sterile filtration of human plasma IgG

The combined models were applied to the constant pressure sterile filtration of the human plasma IgG solution to determine if they would provide better fits of the experimental data than other models. Three experiments were performed using the 13 mm membrane holders. The permeate volume was measured as a function of time until the flux had declined 95% from its initial value of 1.13×10^{-3} m/s.

The permeate volume versus time data was fit using the combined models and all other typical fouling models. The best fit was determined by minimizing the sum of squared residuals (SSR) where the residual was equal to the difference between a data point and the model prediction. Often when the standard blocking model is used both the slope and intercept values are fit to the experimental data. This use of two fitted parameters allows

Table 2
Summary of the five constant flow combined fouling models

Model	Component mechanisms	Equation	Fitted parameters
Cake-complete (Eq. (28))	Cake filtration, complete blocking	$\frac{P}{P_0} = \frac{1}{(1-K_b t)}\left(1 - \frac{K_c J_0^2}{K_b}\ln(1-K_b t)\right)$	K_c (s/m^2), K_b (s^{-1})
Cake-intermediate (Eq. (30))	Cake filtration, intermediate blocking	$\frac{P}{P_0} = \exp(K_i J_0 t)\left(1 + \frac{K_c J_0}{K_i}(\exp(K_i J_0 t) - 1)\right)$	K_c (s/m^2), K_i (m^{-1})
Complete-standard (Eq. (31))	Complete blocking, standard blocking	$\frac{P}{P_0} = \frac{1}{(1-K_b t)\left(1+\frac{K_s J_0}{2K_b}\ln(1-K_b t)\right)^2}$	K_b (s^{-1}), K_s (m^{-1})
Intermediate-standard (Eq. (32))	Intermediate blocking, standard blocking	$\frac{P}{P_0} = \frac{\exp(K_i J_0 t)}{\left(1-\frac{K_s}{2K_i}(\exp(K_i J_0 t)-1)\right)^2}$	K_i (m^{-1}), K_s (m^{-1})
Cake-standard (Eq. (29))	Cake filtration, standard blocking	$\frac{P}{P_0} = \left(\left(1 - \frac{K_s J_0 t}{2}\right)^{-2} + K_c J_0^2 t\right)$	K_c (s/m^2), K_s (m^{-1})

Table 3
Error of fit and model parameters for the cake-complete model, complete model, intermediate model, cake model and standard model

Model	Model fit error, SSR	Fit parameter values
Cake-complete (Eq. (16))	1.12×10^1	$K_b = 2.56 \times 10^{-3}$ s^{-1}, $K_c = 1.30 \times 10^3$ s/m^2
Standard	1.39×10^1	$K_s = 3.88$ m^{-1}
Complete	1.12×10^2	$K_b = 2.90 \times 10^{-3}$ s^{-1}
Intermediate	1.64×10^2	$K_i = 6.01$ m^{-1}
Cake	7.25×10^2	$K_c = 1.35 \times 10^4$ s/m^2

Data for 10 mg/mL human plasma IgG run at 10 psi through 0.22 μm Durapore membrane.

good data fitting but causes a new value of the initial filter flux, J_0, to be determined for each experiment. This is not a physically realistic assumption because the initial permeability is a physical characteristic of the membrane and not the stream. In this study only the parameter K_s was fit to the data. The data and model predictions for one of the samples are shown in Figs. 4 and 5. The data from the other two experiments were similar.

The best fit of the data occurred with the combined cake-complete model, which had and SSR value slightly lower than the standard model, as shown in Table 3. Though the combined cake-complete model does benefit from the use of two fitted parameters the model was better than the other two-parameter models that were developed and tested. The fits of the standard model alone were as good as the fits of the standard model combined with the complete blocking model, Eq. (18), the intermediate blocking model, Eq. (19), or the cake filtration model, Eq. (23). The fit of the intermediate model was as good as the fit of the combined intermediate blocking-cake filtration model, Eq. (17).

The contributions of complete blocking and caking to the combined model were evaluated from the values of K_c and K_b. The terms $K_c J_0$ and K_b/J_0 from Eq. (16) have units of m^{-1} and will be of similar magnitude when their contributions to the combined model are similar. The value of the ratio $K_c J_0^2 / K_b$ was 0.645, indicating that the contributions of the two component models were similar.

4.2. Constant flow: sterile filtration of human plasma IgG

The combined models were applied to the constant flow sterile filtration of the human plasma IgG solution. Three experiments were performed where the pressure was measured as a function of time while pumping the solution at

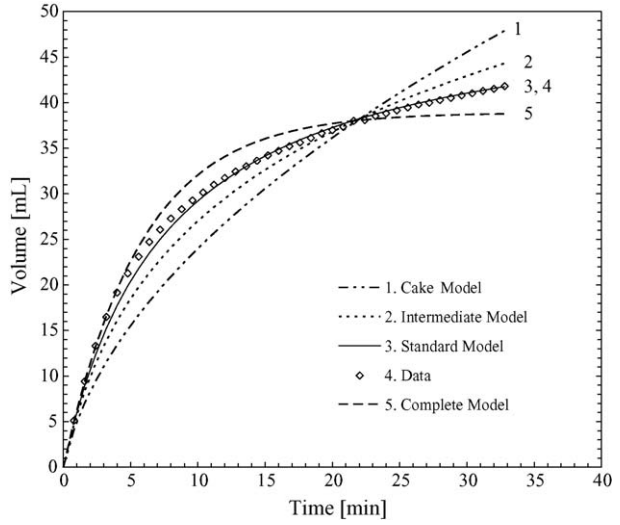

Fig. 4. Volume vs. time data compared to the complete model, intermediate model, cake model and standard model predictions with 10 mg/mL human plasma IgG run at 10 psi through 0.22 μm Durapore membrane.

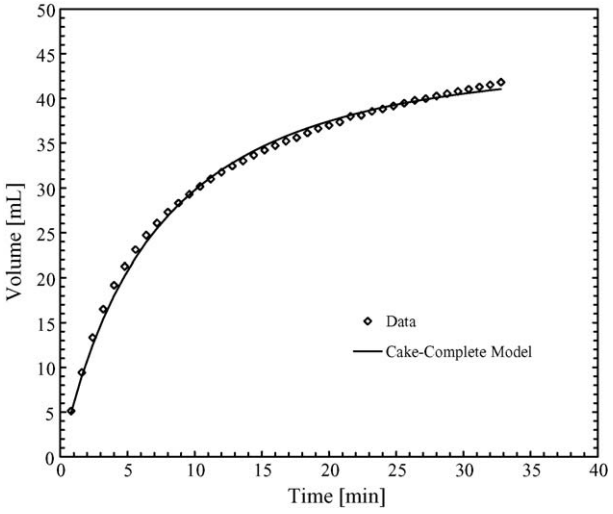

Fig. 5. Volume vs. time data compared to the cake-complete model predictions with 10 mg/mL human plasma IgG run at 10 psi through 0.22 μm Durapore membrane.

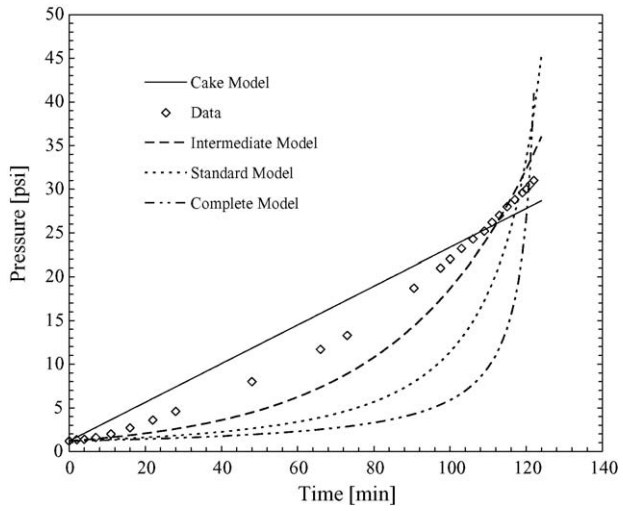

Fig. 6. Pressure vs. time data fit with the typical blocking models: the intermediate model, complete model, cake model, and standard model. Data for 10 mg/mL human plasma IgG run at 579 L/m^2 h through 0.22 μm Durapore membrane.

579 L/m^2 h through membrane samples in 47 mm membrane holders.

The pressure versus time data was fit to one of the experimental data sets using the combined models and all other typical fouling models. The data from the other two experiments were similar. The best fit was determined by minimizing the SSR. The data is fit with the typical models in Fig. 6 and fit with the combined models in Fig. 7.

The best fit of the data occurred with the combined cake-intermediate model, which had and SSR value slightly lower than the cake-complete model, as shown in Table 4. The three combined models provided far better fits than the typical models. The fit of the standard model was as good as the fits of the standard model combined with the complete blocking model, Eq. (31). The fit the intermediate blocking model was as good as the fit of the intermediate model combined with the standard model, Eq. (32).

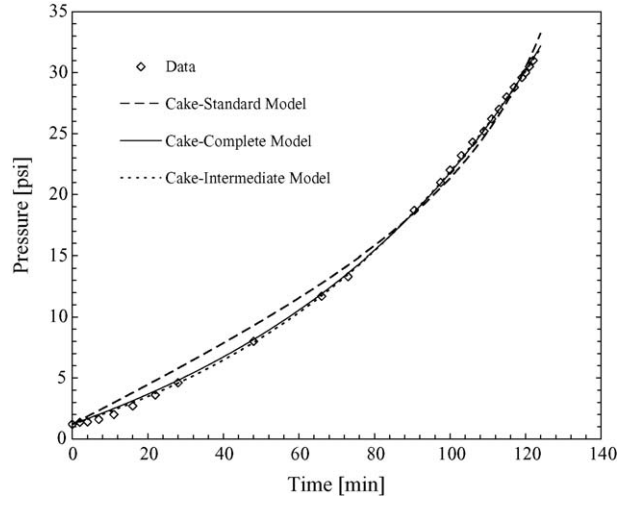

Fig. 7. Pressure vs. time data fit with the combined models: the cake-complete model, cake-standard model, and cake-intermediate model. Data for 10 mg/mL human plasma IgG run at 579 L/m^2 h through 0.22 μm Durapore membrane.

Table 4
Error of fit and model parameters for the cake-intermediate model, cake-complete model, cake-standard model, cake model, intermediate model, standard model and complete model

Model	Model fit error, SSR	Fit parameter values
Cake-intermediate (Eq. (30))	0.58	$K_i = 0.526\ m^{-1}$, $K_c = 4.93 \times 10^4\ s/m^2$
Cake-complete (Eq. (28))	1.36	$K_b = 5.73 \times 10^{-5}\ s^{-1}$, $K_c = 5.74 \times 10^4\ s/m^2$
Cake-standard (Eq. (29))	1.35×10^1	$K_s = 1.67\ m^{-1}$, $K_c = 7.82 \times 10^4\ s/m^2$
Cake	1.12×10^2	$K_c = 1.19 \times 10^5\ s/m^2$
Intermediate	1.44×10^2	$K_i = 2.84\ m^{-1}$
Standard	9.80×10^2	$K_s = 1.40\ m^{-1}$
Complete	2.73×10^3	$K_b = 1.33 \times 10^{-4}\ s^{-1}$

Data for 10 mg/mL human plasma IgG run at 579 L/m^2 h through 0.22 μm Durapore membrane.

The contributions of the component models to the combined models were evaluated from the magnitudes of the fitted parameters. The terms K_cJ_0, K_i, K_s and K_b/J_0 have units of m^{-1} and will be of similar magnitude when their contributions to the combined models are similar. The value of the ratio $K_cJ_0^2/K_b$ was 26.0, K_cJ_0/K_i was 15.1, and K_cJ_0/K_s was 10.5 indicating that caking was a major component of each of the combined models.

4.3. Constant pressure: virus filtration of BSA

The combined models were applied to the viral filtration of a pure protein solution to determine if they would provide better fits of the experimental data than other models. The BSA solution was filtered at a constant pressure through five samples of Viresolve 180 membrane in the 47 mm membrane holders. The permeate volume was measured as a function of time until the flux had declined 98% from its initial value of 3.58×10^{-4} m/s.

The permeate volume versus time data was fit using the combined models and all other typical fouling models. The data was similar for the five experiments. The average and standard deviation was calculated at each time point. The data and model fits are shown in Fig. 8 for the four typical models, and in Fig. 9 for the combined models.

The three combined models provided far better fits of the data than typical blocking models. The cake-complete and cake-intermediate models provided a very good fit of the data in Fig. 9. The fit of the cake-intermediate model was slightly better than that of the cake-complete model, as shown in Table 5, though the fits of the two models were within the standard deviation of most data points. The standard model combined with the cake model provided a fit that was not as good as the other two combined models in Fig. 9, but better than the four typical models in Fig. 8. Table 5 contains the fit error of the different models and allows comparison of the different models. The standard model combined the complete blocking model, Eq. (18), provided the same fit as the standard model alone and is not shown in Fig. 9. The standard model combined with the intermediate model, Eq. (19), provided the same fit as the intermediate model alone and is not shown in Fig. 9.

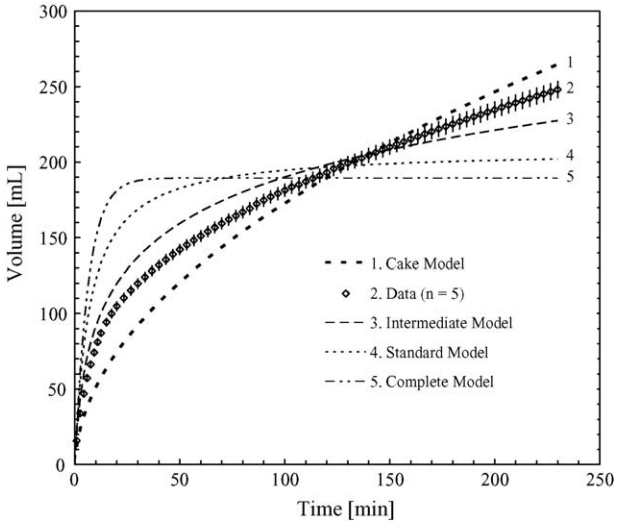

Fig. 8. Volume vs. time data compared to the intermediate model, complete model, cake model, and standard model predictions with 2.5 mg/mL BSA filtered through Viresolve 180 membrane at 30 psi. The data is the average of five runs and the error bars are one standard deviation.

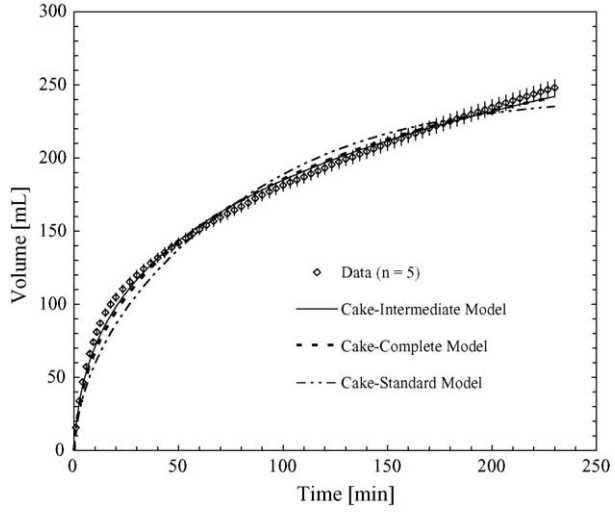

Fig. 9. Volume vs. time data compared to the cake-complete model, cake-standard model, and cake-intermediate model predictions with 2.5 mg/mL BSA filtered through Viresolve 180 membrane at 30 psi. The data is the average of five runs and the error bars are one standard deviation.

Table 5
Error of fit and model parameters for the cake-intermediate model, cake-complete model, cake-standard model, intermediate model, cake model, standard model and complete model

Model	Model fit error, SSR	Fit parameter values
Cake-intermediate (Eq. (17))	9.59×10^2	$K_i = 6.79\ m^{-1}$, $K_c = 2.26 \times 10^5\ s/m^2$
Cake-complete (Eq. (16))	1.62×10^3	$K_b = 1.38 \times 10^{-3}\ s^{-1}$, $K_c = 3.05 \times 10^5\ s/m^2$
Cake-standard (Eq. (23))	6.27×10^3	$K_s = 0.183\ m^{-1}$, $K_c = 4.81 \times 10^5\ s/m^2$
Intermediate	1.13×10^4	$K_i = 30.5\ m^{-1}$
Cake	1.82×10^4	$K_c = 7.21 \times 10^5\ s/m^2$
Standard	7.23×10^4	$K_s = 13.2\ m^{-1}$
Complete	1.32×10^5	$K_b = 2.61 \times 10^{-3}\ s^{-1}$

Data for 2.5 mg/mL BSA filtered through Viresolve 180 membrane at 30 psi.

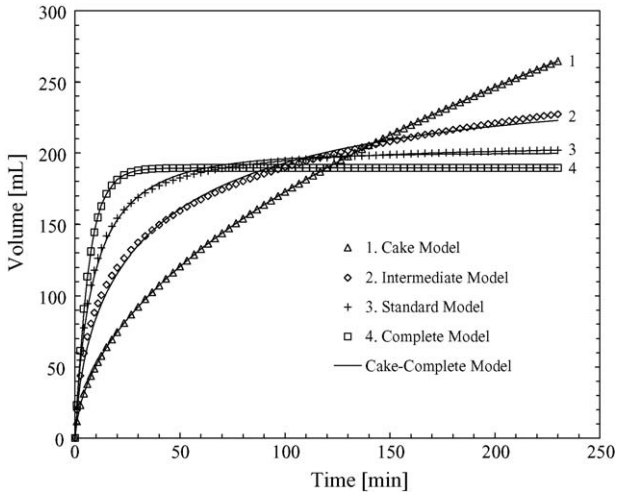

Fig. 10. Cake-complete model (solid lines) fit to predictions of the complete blocking, standard blocking, intermediate blocking and cake filtration model (symbols) for 2.5 mg/mL BSA filtered through Viresolve 180 membrane at 30 psi.

The contributions of the component models to the combined models were evaluated from the magnitudes of the fitted parameters. The value of the ratio $K_c J_0^2 / K_b$ was 28.3, $K_c J_0 / K_i$ was 11.9, and $K_c J_0 / K_s$ was 15.8, indicating that caking was a major component of each of the combined models.

The ability of the combined cake-complete model to provide the best fits of both the sterile filtration data and nearly the best fit of the virus filtration data indicates it will be useful for fitting data from a wide range of solutions and membrane types and be useful for membrane area sizing. This is demonstrated in Fig. 10 where the combined cake-complete model is fit to predictions of each of the typical blocking models from Fig. 8. The cake-complete predictions are identical to either the complete blocking model or cake filtration model when one of the two fitted parameters is small, as expected.

It is interesting that the combined cake-complete model is able to make predictions that are nearly identical to those of the standard or intermediate blocking models. This indicates that the combined cake-complete model will be useful for fitting data that resembles any of the four models. The cake-standard and cake-intermediate models were not as useful for fitting the predictions of the typical blocking models. They only provide improved fits of data that falls between the curves of their respective individual component models. They cannot fit data that resembles the complete blocking model predictions where the flux declines more slowly than other models initially, and more rapidly later in the run.

5. Conclusions

To account for the combined effects of different individual fouling mechanisms, five new fouling models were generated. Explicit equations were derived from Darcy's law that related pressure to time during constant flow operation and volume to time during constant pressure operation. The models used two

parameters and reduced to the equations for the individual models in the absence of the second fouling mechanism.

Generally there is a balance between physical detail and numerically complexity in every theoretical model. The models derived in this study are less physically detailed than the model of Ho and Zydney and will therefore be less useful for estimation of physical parameters. The new combined models, however, are more numerically simple to implement. They have two fitted parameters and provide analytical equations to calculate volume or pressure as a function of time.

The applicability of the models to data for the sterile filtration of IgG and the viral filtration of BSA was tested. The combined caking and complete blockage model was the most useful, as it was able to provide good fits of all data sets, and provide good fits of each of the other individual model predictions. Though providing a good data fit does not prove that fouling occurs by the simultaneous effects of pore blockage and cake formation, the cake-complete model can be viewed as a useful phenomenological equation. The cake-complete model will provide good fits of a broad range of curves where the flux declines in a manner between the extremes of cake filtration and complete blocking. The combined cake-standard and cake-intermediate models also provided good data fits and may be applicable to systems where these models are consistent with the experimentally observed fouling mechanisms.

Nomenclature

A	available membrane frontal area (m^2)
A_0	initial membrane frontal area (m^2)
J	flux (m/s)
J_0	initial flux (m/s)
J'	flux relative to available membrane area (m/s)
K_b	complete blocking constant (s^{-1})
K_c	cake filtration constant (s/m^2)
K_i	intermediate blocking constant (m^{-1})
K_s	standard blocking constant (m^{-1})
P	pressure (kg/ms^2)
Q	flow rate (m^3/s)
R	resistance to filtration (m^{-1})
R_0	initial resistance to filtration (m^{-1})
t	time (s)
V	volume filtered (m^3/m^2)
V'	volume filtered through available membrane area (m^3/m^2)

Greek letters

α	placeholder in cake filtration-standard blocking model
β	placeholder in cake filtration-standard blocking model
μ	solution viscosity (kg/ms)

References

[1] H.P. Grace, Structure and performance of filter media, AIChE J. 2 (1956) 307.
[2] J. Hermia, Constant pressure blocking filtration laws-application to power-law non-Newtonian fluids, Trans. IChemE. 60 (1982) 183.
[3] W.R. Bowen, Q. Gan, Properties of microfiltration membranes: flux loss during constant pressure permeation of bovine serum albumin, Biotechnol. Bioeng. 38 (1991) 688.
[4] A.D. Marshall, P.A. Munro, G. Trägårdh, The effect of protein fouling in microfiltration and ultrafiltration on permeate flux, protein retention and selectivity: a literature review, Desalination 91 (1993) 65.
[5] M. Hlavacek, F. Bouchet, Constant flowrate blocking laws and an example of their application to dead-end microfiltration of protein solutions, J. Membr. Sci. 82 (1993) 285.
[6] E.M. Tracey, R.H. Davis, Protein fouling of track-etched polycarbonate microfiltration membranes, J. Colloid Interf. Sci. 1676 (1994) 104.
[7] W.R. Bowen, J.I. Calvo, A. Hernandez, Steps of membrane blocking in flux decline during protein microfiltration, J. Membr. Sci. 101 (1995) 153.
[8] C. Tien, Granular Filtration of Aerosols and Hydrosols, Butterworths, Stoneham, MA, 1989.
[9] C. Ho, A.L. Zydney, A combined pore blockage and cake filtration model for protein fouling during microfiltration, J. Colloid Interf. Sci. 232 (2000) 389.
[10] R.W.D. Nickalls, A new approach to solving the cubic: Cardan's solution revealed, Math. Gazzette 77 (1993) 354.